International Journal of Biological Macromolecules 299 (2025) 140265

Contents lists available at ScienceDirect

International Journal of Biological Macromolecules

journal homepage: www.elsevier.com/locate/ijbiomac

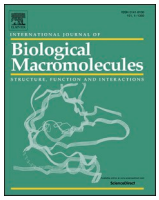

Elucidating the physicochemical interactions between fibrinogen and surfactant mixtures: Implications for pharmaceutical sciences

Ramón Rial *, Michael González-Durruthy, Juan M. Ruso

Soft Matter and Molecular Biophysics Group, Department of Applied Physics and Institute of Materials (iMATUS), University of Santiago de Compostela, 15782 Santiago de Compostela, Spain

ARTICLE INFO

Keywords:
Fibrinogen
Dicloxacillin
CTAB
Molecular docking
Spectroscopic analysis
Protein-ligand interaction

ABSTRACT

This study investigates the physicochemical interactions between fibrinogen (Fib), a key glycoprotein in blood clotting, and a mixture of two biologically active compounds: dicloxacillin (Diclox), an antibiotic; and cetyltrimethylammonium bromide (CTAB), a cationic surfactant. Understanding these interactions is crucial for enhancing drug delivery systems and optimizing pharmaceutical formulations. Molecular docking simulations and various spectroscopic techniques, including UV–Vis, fluorescence, and circular dichroism, were employed to explore how this mixture affects the structural and functional properties of fibrinogen. The docking results revealed that the binding affinity of the dicloxacillin-CTAB mixture with fibrinogen was stronger than either compound individually, suggesting a synergistic interaction. Spectroscopic analysis confirmed structural modifications in the fibrinogen molecule, notably in α-helix content and aromatic residues, indicating loosening or unfolding in protein conformation upon ligand binding. Thermodynamic analyses further supported that the binding process was driven by hydrophobic interactions and electrostatic forces, contributing to stable complex formation. This study advances the current understanding of protein-ligand interactions by exploring the synergistic effects of a dual-ligand system, a novel approach that has not been comprehensively explored in previous literature. These findings provide new insights into the design of drug delivery systems, offering potential applications for improving the efficacy and safety of pharmaceutical formulations targeting fibrinogen-related conditions.

1. Introduction

The dynamic interactions between proteins and surfactants at the molecular interface capture the essence of modern advancements in medicine and pharmacy. This interaction, central to the basic foundations in modulating drug behavior and bioavailability, is essential for unlocking novel therapeutic approaches and optimizing pharmaceutical formulations [1–4]. It is this relevance that has led to protein-surfactant interactions receiving enormous attention [5–8]. However, proteins and surfactant mixtures have attracted less interest. Understanding the interactions between these mixtures and proteins is crucial due to their potential impact on the efficacy, stability, and safety of pharmaceutical formulations, which can affect therapeutic outcomes.

Previous studies have examined how protein-surfactant mixtures affect interfacial tension, viscoelasticity, surface properties, and foam stability, thereby improving the understanding of the fundamental molecular interactions involved [9,10]. Other studies have investigated ionic interactions and the influence of the isoelectric point by developing theoretical models based on thermodynamics and statistical mechanics, which can effectively reproduce experimental observations [11,12]. However, research on the bulk properties of these systems is still limited. A study was conducted to investigate the solubilization of solid protein-surfactant complex salts using a secondary surfactant. The study found that catanionic associations play a predominant role over protein-surfactant interactions [13]. Another investigation was conducted to explore the phase behavior in aqueous two-phase systems that incorporate mixtures of cationic and anionic surfactants, shedding light on the importance of surfactant ratios, electrostatic interactions, and protein partitioning [14]. Efforts have also been made to discern the effects of substituting hydrogen atoms for fluorine atoms in these systems [15]. Additionally, studies focusing on the interaction of small molecules with proteins have provided valuable insights into the binding and modulation of protein structure and function, which is crucial for understanding the behavior of protein-surfactant mixtures. Such

* Corresponding author.
E-mail address: ramon.rial@usc.es (R. Rial).

https://doi.org/10.1016/j.ijbiomac.2025.140265
Received 22 November 2024; Received in revised form 15 January 2025; Accepted 22 January 2025
Available online 23 January 2025

research has demonstrated how small molecules can influence protein dynamics, potentially impacting the efficacy and stability of pharmaceutical formulations [16–19]. Also noteworthy is the method developed to create magnetic carbon nanotubes (MCNTs) that can bind and stabilize DNA and proteins using catanionic surfactants to enhance the electrostatic interaction between biomolecules and MCNTs, facilitating their rapid migration and compaction [20].

Building upon this foundation, the present study investigates the physicochemical interactions between fibrinogen and a mixture of two biologically active compounds: dicloxacillin, cetyltrimethylammonium bromide. Fibrinogen, a soluble plasma glycoprotein, plays an indispensable role in the hemostatic system of the human body, acting as a precursor of fibrin during the blood clotting process. In addition to its role in wound healing, it also serves as a scaffold for cellular components involved in tissue repair, acting as a ligand for several cell surface receptors. This interaction influences cell adhesion, migration, and proliferation, essential steps in the inflammatory response and tissue repair. In addition, the plasma concentration of fibrinogen can increase significantly in response to inflammation, tissue injury, or infection, making it a marker for cardiovascular risk and other diseases. The structure of fibrinogen consists of three pairs of polypeptide chains (Aα, Bβ, and γ), linked together by disulfide bonds. The two D regions, located at the ends of the fibrinogen molecule, are well connected to the E-region by coiled-coil segments. Each D region includes the C-termini of the Bβ and γ chains and is involved in lateral aggregation and stabilization of the fibrin clot. These regions facilitate the formation of a stable, three-dimensional fibrin network by promoting interactions between fibrin monomers, thereby enhancing the mechanical properties and resistance of the clot to fibrinolysis [21]. This structure provides a versatile platform for interactions with various molecules, including surfactants, that can alter its functionality and stability [22,23]. For their part, dicloxacillin and CTAB (Cetyltrimethylammonium Bromide) are two compounds with distinct chemical properties and uses in the pharmaceutical and biochemical fields. Dicloxacillin is a semi-synthetic penicillin antibiotic that belongs to the penicillinase-resistant group of beta-lactam antibiotics. It is specifically designed for penicillin-resistant Gram-positive bacteria, effective in treating skin infections, and pneumonia. In the context of pharmaceuticals, its main use is therapeutic [24,25]. On the other hand, CTAB, a quaternary ammonium compound, is a cationic surfactant widely used in pharmaceutical formulations, cosmetic products, and as a reagent in molecular biology. CTAB's surfactant properties make it valuable for its ability to solubilize drugs, enhance the permeability of active pharmaceutical ingredients through biological membranes, and stabilize formulations. Additionally, in molecular biology, CTAB is employed in the extraction and purification of DNA and RNA due to its ability to precipitate nucleic acids. Its broad spectrum of applications underscores its versatility and importance across multiple scientific and industrial fields. The commonality between dicloxacillin and CTAB in biological contexts lies in their ability to interact with biological systems, albeit through vastly different mechanisms: dicloxacillin as an antibiotic agent targeting specific bacteria, and CTAB as a surfactant enhancing drug delivery and stability [26–29].

Given the central role of fibrinogen in essential physiological processes and its potential in therapeutic contexts, the study of its interactions with various molecules, particularly surfactants, offers a promising avenue for advancing medical and pharmaceutical innovations. Such investigations lay a strong foundation for developing innovative strategies to address a wide range of medical conditions. As a result, exploring the interplay between fibrinogen and the combination of dicloxacillin and CTAB holds significant potential for uncovering insights that could refine drug delivery systems. This research aims to enhance both the efficacy and safety of pharmaceutical formulations, ultimately guiding the design of more effective and safer therapeutic solutions.

2. Materials and methods

2.1. Reagents

Hexadecyltrimethylammonium bromide (CTAB, 99 %, ref. n. H5882), sodium dicloxacillin [3-(2,6-dichlorophenyl)–5–methyl–4-Isoxazolyl penicillin] (ref. n. D9016) and bovine plasma fibrinogen, fraction I, type IV, (No. 9001-32-5) were obtained from Sigma. The buffer solution used for fibrinogen was 50 mM glycine plus sodium hydroxide to achieve a pH of 8.5. Samples were freshly prepared for each experiment 1 h prior to use. Solutions were made using triple-distilled and degassed water.

2.2. Molecular docking and conformational drug-drug interaction network

A molecular docking approach was executed by using AMDock, a software tailored for proficient prediction of protein-ligand binding modes and ΔG binding affinities (kcal/mol). AMDock's methodology amalgamates a genetic algorithm with a grid-based strategy [30]. The preliminary phase necessitated the preparation of the fibrinogen receptor and the ligand structures of the binary catanionic mixture, specifically dicloxacillin (PubChem CID: 18381; MW: 470.3 g/mol) and hexadecyltrimethylammonium bromide–CTAB (PubChem CID: 5974; MW: 364.4 g/mol) [31]. For the fibrinogen structure (*RCSB Protein Data Bank* (PDB) X-ray structures [32], i.e. with *PDB ID*: 1DEQ) [33] co-crystalized ligands and water molecules were excised. The dicloxacillin and CTAB structures forming the mixture were primed by allocating Gasteiger charges and optimizing geometries. The AMDock algorithm employs a hybrid scoring function, amalgamating various energy force field terms, to assess the ligand's binding affinity across diverse orientations and conformations. For discerning the paramount binding mode based on individual ligand conformations ($N = 10$ conformations) and the binary mixture, AMDock adopts a hierarchical simulation protocol [30]. This commences with a coarse-grained search via an FFT-based technique, succeeded by a refinement phase leveraging a Monte Carlo algorithm. Subsequent to docking, the predicted conformational binding modes and ΔG affinities values undergo further scrutiny and validation through an array of post-docking analytical tools aiming to further construction of the conformational drug-drug interaction network in three simulation conditions i) dicloxacillin conformational drug-drug interaction network, ii) CTAB conformational drug-drug interaction network, and iii) mixture dicloxacillin plus CTAB conformational drug-drug interaction network [30].

2.3. UV–vis absorption spectra

UV–visible absorption spectra were obtained using a Cary 100 Bio UV–Vis Spectrophotometer (Agilent Technologies, USA) within a wavelength range of 225–400 nm. A standard solution of fibrinogen, at a concentration of 0.07 mM, served as the reference for UV measurements. To assess the individual absorbance effects of each compound, solutions of pure dicloxacillin and CTAB were incrementally introduced in concentrations between 0.083 mM and 0.83 mM, ensuring a consistent fibrinogen concentration. Additionally, mixtures with equal concentrations of both ligands were introduced to the 0.07 mM protein solution. The absorbance values were corrected for the corresponding blanks to eliminate any potential baseline interference. Each measurement was conducted in duplicate to validate accuracy and reduce potential errors. The observed replicates exhibited negligible variation, with the reported data reflecting the average of both measurements.

2.4. Fluorescence emission spectra

Fluorescence emission spectra were obtained using a Cary Eclipse spectrofluorometer (Agilent Technologies, USA), with both excitation

and emission slits calibrated to 5 nm. All measurements were conducted at a controlled temperature of 298 K. Measurements were taken at 0.5 nm intervals, averaging over a 0.5 s duration. The excitation was consistently set at 280 nm, and the spectral analysis spanned from 250 to 550 nm. To account for inner filter effects and ensure accurate quenching results, corrections were applied using the formula: $F_{corr} = F_{obs} \times 10^{[(A_{exc}+A_{em})/2]}$, where F_{corr} and F_{obs} denote the corrected and observed fluorescence intensities, respectively. A_{exc} and A_{em} represent the system's absorptions at the excitation and emission wavelengths, respectively. Data analysis was facilitated by the UV–Vis-IR Spectral Software (FluorTools) [34].

For thermodynamic analysis of the ternary complex formation, fluorescence quenching measurements were conducted at three specified temperatures (e.g., 298 K, 303 K, and 308 K) to apply the van't Hoff equation, enabling calculation of thermodynamic parameters. The fluorescence spectra of the fibrinogen-catanionic compound complexes were examined in a manner analogous to the UV–Vis approach. Initially, each ligand was added individually, followed by the combined catanionic mixture, with ligand concentrations ranging between 0.083 mM and 0.83 mM.

2.5. Circular dichroism (CD)

Utilizing a JASCO-715 spectropolarimeter (Jasco, Japan) equipped with a JASCO PTC-343 Peltier-regulated cell holder, Far-UV circular dichroism (CD) spectra were acquired. Quartz cuvettes possessing a pathlength of precisely 0.2 cm were employed. The spectral range was recorder between 190 and 280 nm for both pure protein and ligand solutions. The protein sample was 1 mg/mL, corresponding to a molarity of 0.02 mM. Concurrently, a mixture of dicloxacillin and CTAB was added, with concentrations ranging from 0.83 to 4.2 mM for both compounds. Instrumental parameters were meticulously set: a resolution and bandwidth both at 1 nm, sensitivity calibrated at 50 mdeg, a response interval of 8 s, an accumulation factor of 3, and a scanning velocity of 50 nm/min. Any absorbance attributable to the buffer methodically negated, adhering to the instrumental parameters. Experimental data were expressed in terms of molar ellipticity by the equation $[\theta]_\lambda = \theta_\lambda M_r/ncl$, where M_r is the molecular weight of the protein, n represents residue quantity, c is the protein concentration, l corresponds to the cuvette's path length, and θ_λ is the ellipticity at a wavelength λ given by the apparatus. The resultant CD profiles represent the composite spectra inherent to α-helix, β-sheet, β-turn, and random coil configurations. Subsequent analysis of secondary structure composition was conducted using the webserver BeStSel software [35].

3. Results and discussion

3.1. Computational approach

To investigate the molecular interactions involved, the primary aim was to theoretically elucidate the effects of the CTAB/dicloxacillin mixture on its interaction with fibrinogen. This was achieved through a series of computational methodologies, including: (i) structural modeling of fibrinogen in its unbound state, (ii) evaluation of the

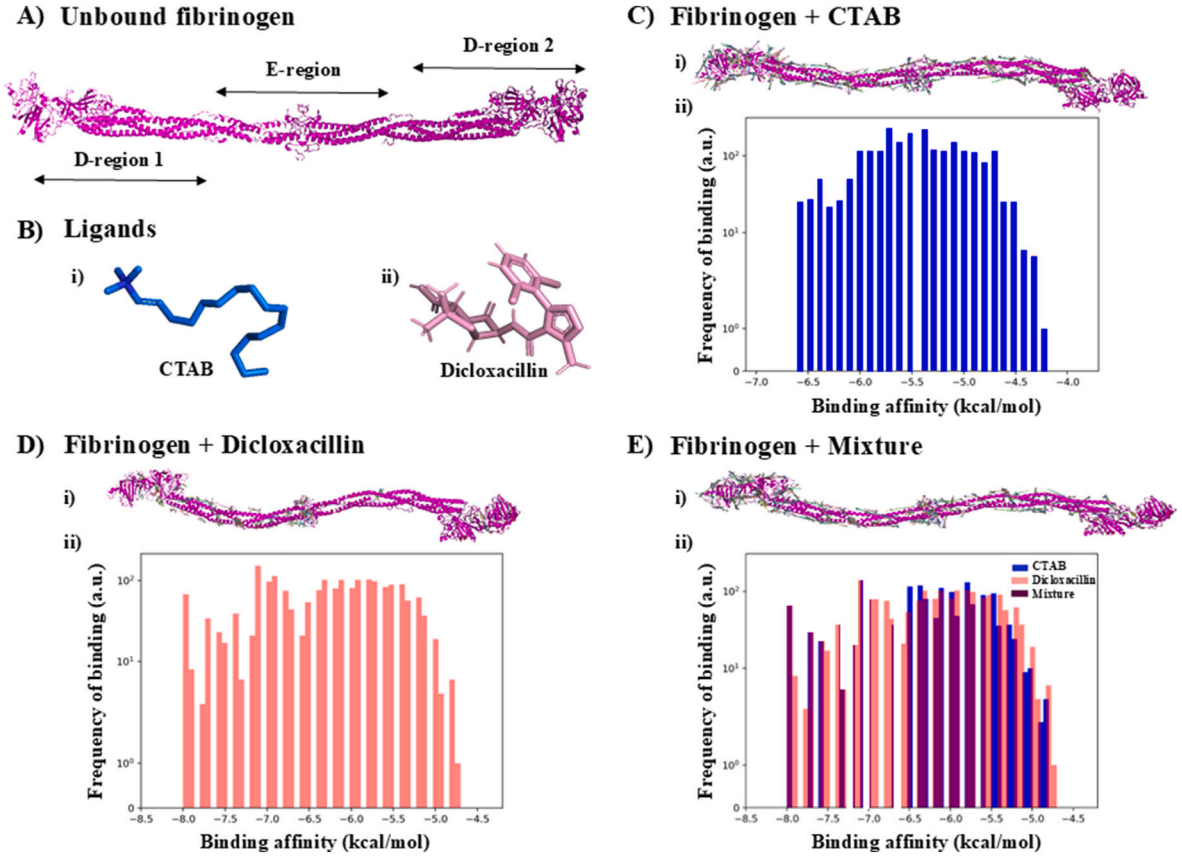

Fig. 1. A) Representation of the crystallographic 3D-structure of unbound fibrinogen highlighting relevant structural segments (E-region > D-region 1 > D-region 2) directly involved in its propensity to bind ligands (i.e., dicloxacillin, CTAB, and the mixture of dicloxacillin plus CTAB). B) Chemical structures of the evaluated ligands: i) CTAB, ii) Dicloxacillin. Next, 3D-structural views for (i) generated docking complexes obtained from blind docking modeling (above) with the corresponding bar-plot (ii) showing the relationship between the binding affinity ΔG (kcal/mol) vs. frequency of binding (below) considering the three docking conditions evaluated in this study: C) fibrinogen plus CTAB (labeled-blue bars), D) fibrinogen plus dicloxacillin (labeled-pink bars), and E) fibrinogen plus mixture CTAB/Diclox (labeled-dark red bars).

thermodynamic binding affinity (ΔG, kcal/mol) in conjunction with the binding frequency for isolated docking systems (fibrinogen with CTAB and fibrinogen with dicloxacillin), and (iii) modeling of the binding affinity for mixed docking systems (fibrinogen in the presence of the CTAB/dicloxacillin mixture). The results of these analyses are presented in Fig. 1.

Using Fig. 1A, which represents the unbound state of fibrinogen, as a reference to explain where specific interactions occur in the fibrinogen structure, we ~~can show~~ showed different aspects of the interaction between fibrinogen and evaluated ligands (Fig. 1B) based on the blind docking results. In general terms, both ligands exhibit spontaneous binding interactions from a thermodynamic perspective, as indicated by the negative values for the ΔG affinity of the formed docking complexes.

Specifically, for the case of fibrinogen plus CTAB docking complexes the obtained histogram (labeled blue bars) representing the binding affinity (in kcal/mol) ranges from −7.0 to −4.5 kcal/mol, showing the energy required to form stable interactions [36,37], while the y-axis indicates the frequency of binding occurrences of the CTAB across the fibrinogen structure (Fig. 1C). Similarly, the docking results on the fibrinogen plus dicloxacillin are shown in the Fig. 1D for the case of fibrinogen plus dicloxacillin docking complexes the obtained histogram (labeled pink bars) with binding affinity values ranging from −8.0 to −4.5 kcal/mol, slightly with better affinity (−1 kcal/mol) than the CTAB molecule. Moreover, dicloxacillin showed a higher frequency of binding events that the CTAB in the same theoretical simulation conditions.

In addition, we ~~show~~ analyzed the blind docking results for the mixed system (i.e., fibrinogen plus CTAB/dicloxacillin mixture). Fig. 1E shows three sets of bars: purple for CTAB alone, pink for dicloxacillin alone, and dark purple for their mixture. This comparative analysis highlights the differences in thermodynamic binding behavior when both molecules are present together versus individually. In this case, the ΔG of the CTAB/dicloxacillin mixture interacting with fibrinogen ranged from −8.0 to −4.8 kcal/mol theoretically suggesting that the mixture has a slightly higher affinity than the isolated compounds under the same simulation conditions.

The distinction between individual molecular interactions and those occurring within a mixture is well documented in the literature, where the presence of multiple interacting agents can lead to altered binding affinities and thermodynamic behavior. Singh et al. [38] showed that the interaction between two monoclonal antibodies (mAbA and mAbB) in a mixed system exhibited a synergistic effect, resulting in increased affinity compared to the individual components. This is consistent with our results for the mixture CTAB/dicloxacillin, where the ΔG values indicated a higher affinity for the combined system. Another analysis [39] highlights the limitations of traditional additive models in predicting the effects of chemical mixtures, especially when synergistic or antagonistic interactions occur, as is likely to be the case in our study. Further studies [40] emphasize the challenges of risk assessment when dealing with complex mixtures where the behavior of individual chemicals may change significantly when present in combination, further supporting our observation of increased binding affinity in the CTAB/dicloxacillin system. Finally, the work of Carpenter et al. [41] on environmental mixtures reinforces the idea that external factors and the presence of multiple agents can alter both toxicokinetics and toxicodynamics, leading to deviations from expected individual behaviors; paralleling the thermodynamic changes observed in our mixed system. Taken together, these studies underscore the critical importance of considering mixture-specific interactions when evaluating the binding behavior of compounds.

The docking analysis, further detailed in the Supporting information (SI), reveals distinct edge-to-face aromatic binding profiles regarding the best-ranked conformation-based affinity for CTAB (i.e., conf #11 > conf #3 > conf #9) and dicloxacillin (i.e., conf #9 > conf #10 > conf #13), highlighting the E-region of fibrinogen as the preferred binding region (eg., best-ranked ligand binding sites 1, 2, 3). This finding aligns with prior studies on fibrinogen's structural flexibility and functional importance in fibrin polymerization [42]. The dynamic and exposed nature of the E-region facilitates the accommodation of small molecules, making it a favorable target for both evaluated ligands.

Following this idea, results on 2D-lig-plot interaction diagrams show that, CTAB forms a stable docking conformation with key residues like LEU99-Chain A, PRO69-Chain C, ARG137-Chain B, TYR68-Chain C, and LYS72-Chain C, which primarily engage in hydrophobic and electrostatic interactions. Notably, ARG137-Chain B forms attractive charge interactions with CTAB's quaternary ammonium group, enhancing binding stability. Additionally, weak carbon-hydrogen bonds involving GLN134-Chain B and GLN73-Chain C provide supplementary stabilization. These interactions underscore the role of hydrophobic forces and electrostatic contributions in stabilizing CTAB's long hydrophobic chain within the non-polar environment of the E-region.

Dicloxacillin, on the other hand, demonstrated a slightly stronger binding affinity, driven primarily by conventional hydrogen bonding. Key residues include: ASP66-Chain E, SER48-Chain D, SER48-Chain A, and ARG51-Chain A, which form robust interactions with dicloxacillin's polar functional groups. The involvement of ASP66-Chain E highlights the ionic interaction between its negatively charged carboxylate group and the protonated amine group of dicloxacillin. Hydrophobic interactions involving residues like CYS50-Chain A, VAL79-Chain B, and VAL79-Chain E further stabilize dicloxacillin by interacting with its aromatic and aliphatic regions. More details can be found in Figs. SI1, SI2 and SI3.

The contrasting binding mechanisms of the two ligands reflect their chemical nature. CTAB, a cationic surfactant, predominantly relies on hydrophobic contacts and electrostatic interactions, effectively utilizing the non-polar and charged residues within the E-region. In contrast, dicloxacillin's binding depends more heavily on polar and hydrogen-bond interactions, consistent with its antibiotic properties. These differences highlight the flexibility of the E-region to accommodate diverse ligands through varied interaction types. More details can be found in Figs. SI4, SI5, and SI6.

From this perspective, the slightly higher frequency of binding events in the mixed system (CTAB/dicloxacillin + fibrinogen) compared to the isolated systems (CTAB + fibrinogen and ~~D~~ dicloxacillin + fibrinogen) suggests a more energetically stable docking complex. This thermodynamic stability could theoretically be attributed to the synergistic effects of the two drugs when combined, which may increase their binding affinity to the fibrinogen protein. The influence of the compounds (CTAB and dicloxacillin) under mixture combination interacting with fibrinogen can be rigorously explained by the combination index (CI) parameter proposed by Chou-Talalay [43–47]. The Chou-Talalay method for drug mixture combinations is based on the median effect equation, which is derived from the mass action law principle. This unified theory links single and multiple drug entities, as well as first-order and higher-order interaction dynamics. The Chou-Talalay combination index (CI) theorem quantitatively defines additive effects when (CI = 1), synergism (CI < 1), and antagonism (CI > 1) in drug combinations. In addition, this theory provides algorithms for theoretical simulations to assess synergism and/or antagonism at any level of action and concentration capturing the complexity of mixture interactions.

To visualize the results on the mixture interacting with fibrinogen, the corresponding isobolograms were generated. In this context, an isobologram represents a mechanistic tool which allows to explain specific combination effect linked to the concentrations of two or more compounds (or their conformations) required to achieve the combined effect.

Within this conceptual framework, we have applied the Chou-Talalay combination index (CI) oriented to theoretically explain three relevant aspects: i) identification of interaction mechanism based CI values of the mixture system (CTAB/dicloxacillin + fibrinogen) in the relevant structural segments of fibrinogen (i.e., E-region, D-region 1, and D-region 2), ii) generating the theoretical 2D-isobologram for the mixture system in the same range of experimental concentrations

evaluated, and iii) generating the theoretical 2D-isobologram derived from the combined docking conformations of CTAB and dicloxacillin interacting with fibrinogen protein. This is described in detail in Fig. 2.

Firstly, we evaluated the interaction mechanisms of a mixture of CTAB and dicloxacillin with fibrinogen by analyzing the Combination Index (CI) values across different structural segments of fibrinogen, specifically the E-region, D-region 1, and D-region 2. According to the obtained results, we observed that, for the evaluated mixture (CTAB/dicloxacillin + fibrinogen), the synergistic and additive interactions were theoretically more predominant in D-region 1 and D-region 2 of the fibrinogen molecules. In contrast, antagonistic binding effects were more prevalent in the central E-region of the fibrinogen. These results are supported by the CI values obtained from blind docking over the entire crystallographic structure of the fibrinogen structure, plotted according to the combination index values. See Fig. 2A.

The theoretical isobologram generated by considering the same range of experimental concentrations evaluated by spectroscopic methods strongly suggests that the mixture of CTAB and dicloxacillin exhibits a predominance of synergistic and additive binding effects over antagonistic effects for the mixture as illustrated by the blue labeled region in the isobologram (Fig. 2B). This suggests that within certain concentration ranges for example from 0.14 to 0.24 mM for CTAB and from 0.0007 to 0.001 mM for dicloxacillin reinforcing the idea that the combined effect of CTAB and dicloxacillin enhances the overall interaction with fibrinogen, potentially leading to thermodynamically stable binding complexes. However, as the concentration ranges increased, a transition towards antagonistic binding effects was observed based on the CI values of the interacting mixture represented by the labeled red region of the isobologram (Fig. 2B). This shift indicates that at higher mixture concentrations, the combined effect of CTAB and dicloxacillin may lead blocking binding mechanisms (antagonisms). The identification of these interaction mechanisms is crucial for optimizing the dosage of potential combinations for therapeutic strategies to maximize beneficial effects while minimizing adverse interactions.

Linked to previous theoretical results (shown in Fig. 1), it should be noted that in molecular docking studies, a higher frequency of binding events typically correlates with lower binding energy value ($\Delta G < 0$ kcal/mol), indicating a more stable interaction for most of the ligands and simulation conditions evaluated. Therefore, the mixed system is likely to form a more stable complex with fibrinogen, reducing the overall binding energy of the protein compared to the isolated systems. This increased stability may be due to complementary interactions between CTAB and dicloxacillin, which may create a more favorable synergistic binding environment compared with the antagonistic effects on the fibrinogen molecule. From the structural point of view, the slightly increased stability and binding frequency previously observed for the mixed system could have significant implications for the function of fibrinogen. Fibrinogen is a key protein in the formation of blood clots and its interaction with drugs could affect its ability to form clots. A more stable docking complex formed with the mixture could alter the physiological conformation of the fibrinogen molecule when interacting with the mixture, potentially enhancing or inhibiting its clotting function.

To further explore the conformational aspects, we then decided to generate theoretical 2D isobologram derived for all docking conformations of CTAB and dicloxacillin combinations interacting with the

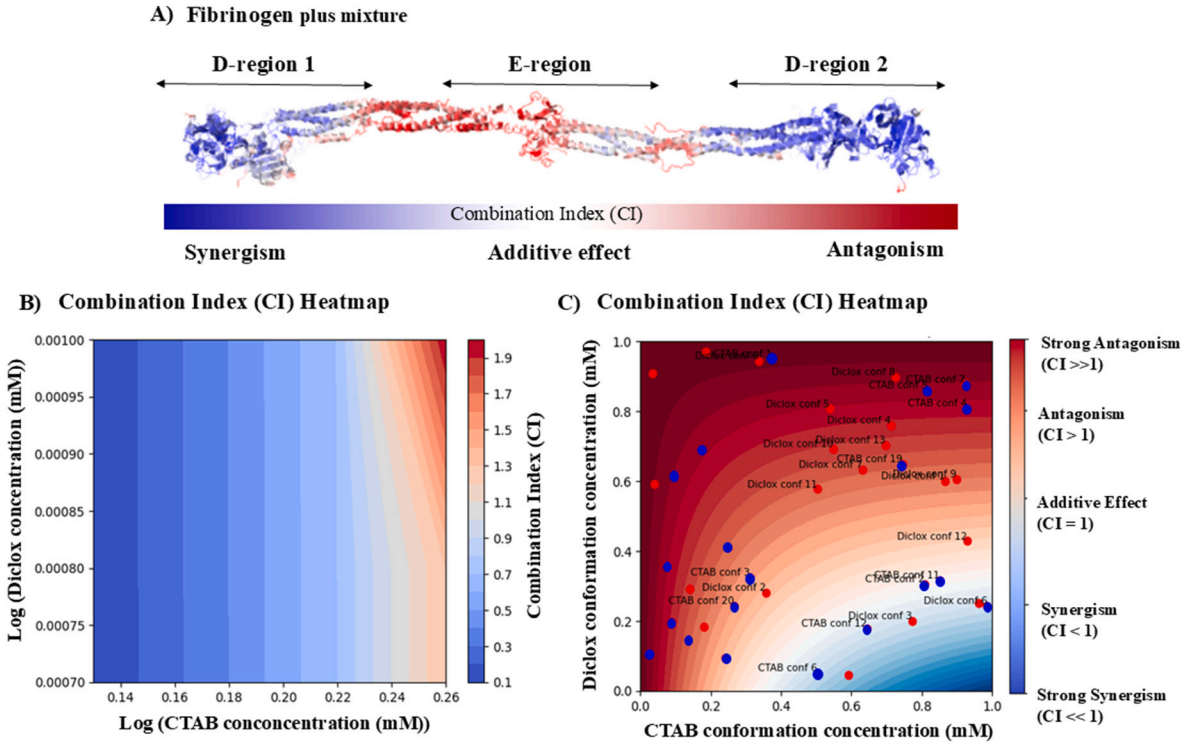

Fig. 2. A) 3D-crystallographic structure of the fibrinogen highlighting relevant structural segments (i.e., E-region, D-region 1, and D-region 2) rendered according to the combination index values obtained after CTAB plus dicloxacillin mixture interaction. The bar color in the bottom is to qualitatively represent the evaluated parameter CI from the mechanistic point of view as synergistic, additive and antagonistic binding according to the color intensity (blue-to-white-red transitions) in the rendered fibrinogen structure. B) Graphical representation of the theoretical 2D-isobologram between CTAB and dicloxacillin under mixture combination with fibrinogen. Herein, only the best-ranked conformations-based on the ΔG binding affinity (i.e., lowest negative ΔG values) were considered for both ligands. The intensity bar color in the right-side of the isobologram is to depict the combination index (CI) of the formed binary mixture as labeled-blue region ($CI_{(CTAB\text{-}Dicloxacillin\ mixture)} < 1$) corresponds to synergistic effects while labeled-red region ($CI_{(CTAB\text{-}Dicloxacillin)} > 1$) corresponds to antagonistic effects. C) Representation of the theoretical 2D-isobologrames based on overall generated conformations between CTAB and dicloxacillin under combination interacting with the fibrinogen protein. Here, the different conformations for CTAB and ~~D~~ dicloxacillin are represented as red and blue circles; respectively scattered in the isobologram heatmap. The intensity bar color in the right-side represents different levels of the synergistic or antagonistic binding effects based on the CI values.

fibrinogen protein (Fig. 2C). In particular, these results revealed a general predominance of strong to moderate antagonistic effects (CI ≫ 1) over strong to moderate synergistic effects (CI ≪ 1) for the CTAB/dicloxacillin mixture when interacting with fibrinogen, highlighting the importance of conformational aspects in anticipating the intensity of these binding mechanisms. The conformational isobologram strongly suggests that some specific conformations of the CTAB and dicloxacillin in the mixture are more likely to induce antagonistic effects with varying intensities, ranging from weak to strong. Conversely, other conformations in the mixture may induce moderate to strong synergistic effects. These observations suggest that allosteric interactions may play a significant role in the interaction of the mixture with the binding sites of fibrinogen, particularly in the E-region, D-region 1, and D-region 2. The influence of binding factors is also suggested by the presence of positive allosteric binding cooperativity, usually determined by the Hill coefficient (n) with positive values.

Both the theoretical isobologram and the experimental Stern-Volmer analysis, which will be discussed in detail later, converge on the idea that specific conformations of the CTAB/dicloxacillin mixture significantly influence the binding mechanism, with cooperative binding effects playing a key role. The observed variation in binding intensity, ranging from antagonistic to synergistic, could be attributed to the involvement of allosteric sites on fibrinogen that modulate ligand interactions across different regions. Furthermore, the study highlights non-linear concentration and conformational dependent binding behavior, as evidenced by the sigmoidal lines within the isobologram (Fig. 2C). This non-linearity highlights the complexity of the interaction mechanisms, where conformational factors significantly influence the binding profile of the mixture.

From the structural point of view of the fibrinogen molecule, if the binding of the drug mixture induces a conformational change that exposes or hides critical binding sites, it could either promote or inhibit the formation of fibrin clots. This could have therapeutic implications, such as improving the efficacy of anticoagulant treatments or enhancing the stability of fibrin clots during wound healing.

A potential limitation of this computational approach is the inherent complexity and variability of biological systems, which may not be fully captured by computational models. Although isobologram analysis provides valuable insights into the conformational and concentration-dependent interactions, it is based on theoretical assumptions that may not account for all biological contexts. In addition, the accuracy of the combination index and the predicted antagonistic or synergistic effects are highly dependent on the quality and completeness of the crystallographic input data of both the protein receptor (fibrinogen) and the ligands (CTAB and dicloxacillin). Furthermore, experimental validation is crucial to confirm the computational predictions, as in vitro and in vivo conditions can introduce variables that are difficult to simulate accurately. Despite these limitations, this computational approach offers a powerful tool to anticipate the potential adverse effects of mixing systems, complementing experimental studies (e.g., spectroscopic). Therefore, we believe that the predictive potential of this theoretical approach for understanding complex mixture interaction mechanisms remains significant in this still largely unexplored field.

3.2. Experimental characterization

3.2.1. Spectroscopic analysis

Measurement via UV–vis absorption offers an immediate means to investigate alterations in protein conformation and complex formation. Fig. 3 illustrates the UV–vis absorption spectra of Fibrinogen in its plain state and in conjunction with CTAB, dicloxacillin and the mixture of catanionic ligands. The spectra demonstrated that fibrinogen exhibits two absorption peaks, notably at 214 nm and 280 nm. The peak at 214 nm is associated with the n-π* electronic transition of peptide bonds within the protein structure, particularly indicative of α-helix conformations. This absorption peak is indicative of the characteristic structure of fibrinogen, with the intensity and wavelength of this peak susceptible to changes induced by alterations in its environment or interactions with ligands. For its part, the absorption peak around 280 nm is attributed to the presence of aromatic amino acid residues, predominantly tryptophan (Trp) and tyrosine (Tyr), within the protein. These residues absorb light in the ultraviolet range due to their aromatic ring structures, rendering them sensitive to changes in their microenvironment.

In this particular case, the intensity peak at 214 nm of fibrinogen demonstrates a consistent diminishment and accompanying red shift in correlation with escalating CTAB concentrations. Conversely, the observed increase in the absorption peak at 214 nm upon the addition of dicloxacillin indicates a significant interaction between dicloxacillin and the fibrinogen protein, leading to changes in the protein's structural environment. The differential responses of the absorption peak at 214 nm to the addition of CTAB and dicloxacillin suggest distinct modes of interaction between the fibrinogen protein and the ligands. The decrease in the absorption peak intensity at 214 nm upon the addition of CTAB is likely indicative of a disruption or alteration of the fibrinogen's native α-helix structure. CTAB is known to interact with proteins through electrostatic interactions, which may potentially lead to protein denaturation or structural perturbations. The decrease in absorption intensity suggests a destabilization of the α-helix motifs within fibrinogen, indicative of structural rearrangements or unfolding induced by CTAB binding. Conversely, the increase in the absorption peak intensity at 214 nm following the addition of dicloxacillin suggests a stabilization or restoration of the α-helix structure within fibrinogen. Dicloxacillin, is likely to form noncovalent bonds with specific amino acid residues within the protein, which may promote the reformation of α-helix motifs or induce structural rearrangements that enhance the absorption at 214 nm. The contrasting effects of CTAB and dicloxacillin on the absorption peak at 214 nm highlight the diverse mechanisms by which ligands can

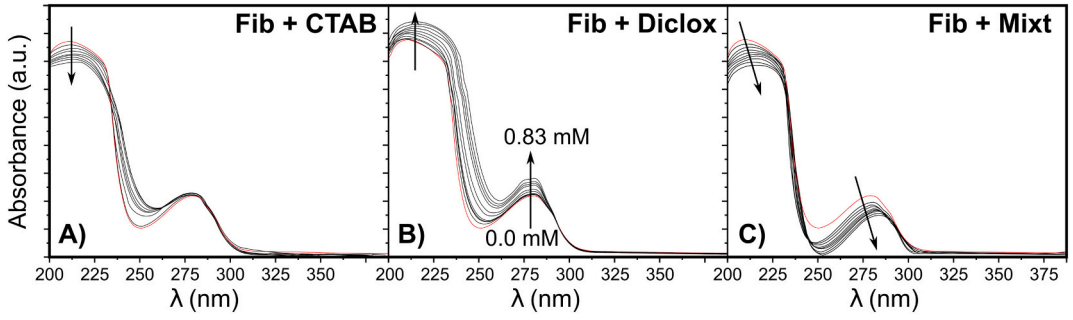

Fig. 3. UV absorption spectra of fibrinogen protein (C_{Fib} = 0.07 mM) with increasing concentrations of ligands: A) fibrinogen + dicloxacillin, B) fibrinogen + CTAB, C) fibrinogen + Mixture CTAB/Diclox. Please note that for all the spectroscopic conditions, increasing concentrations of ligands were established as (C_{Diclox} = C_{CTAB} = mixture CTAB/Diclox (0.083, 0.166, 0.250, 0.330, 0.416, 0.500, 0.580, 0.660, 0.750, 0.830) mM). The reference control is represented by the UV absorption spectra labeled in red for the fibrinogen protein (0.07 mM) in the absence of any evaluated ligands (i.e., Diclox, CTAB, and mixture CTAB/Diclox at 0.00 mM).

modulate the structure and stability of fibrinogen.

Focusing on the peak at 280 nm, Fig. 4 shows a detailed view at a closer range. When CTAB is added, the absorption peak at 280 nm remains largely unaffected, suggesting that CTAB does not induce significant changes in the polarity or hydrophobicity of the microenvironment and indicating that the surfactant may not directly interact with these residues or alter their accessibility. In the case of dicloxacillin, we observe a notable increase in the intensity, meaning that dicloxacillin does induces changes in the microenvironment surrounding the aromatic residues within fibrinogen, potentially by altering the solvent polarity or hydrophobicity or by inducing conformational changes that affect the exposure or arrangement of the aromatic residues. However, when a mixture of both CTAB and dicloxacillin is added, the absorption peak at 280 nm experiences a decrease in intensity and a red shift. This simultaneous alteration suggests a synergistic interaction between CTAB and dicloxacillin, leading to changes in the microenvironment surrounding the aromatic residues that differ from the effects of each ligand individually. The decrease in absorption intensity may indicate a reduction in the polarity or hydrophobicity of the microenvironment. Additionally, the red shift in the absorption peak suggests changes in the electronic environment, potentially resulting from alterations in the ligand-protein interactions or conformational changes induced by the combined presence of both ligands. These observed synergistic effects suggest a complex interplay between the two ligands and the protein. As explained, CTAB, a cationic surfactant, is known to interact with proteins through electrostatic interactions, which may result in alterations to protein conformation or denaturation. In contrast, dicloxacillin, forms bonds with specific amino acid residues within the protein, influencing its structural stability. When both CTAB and dicloxacillin are present, they may compete for binding sites on the fibrinogen protein, leading to altered ligand-protein interactions compared to when each ligand is present alone. This competition could result in changes in the protein's conformational dynamics or stability, affecting both the absorption peak at 214 nm, associated with α-helix structures, and the absorption peak at 280 nm, indicative of the microenvironment surrounding aromatic residues. Furthermore, the simultaneous presence of CTAB and dicloxacillin may result in cooperative effects, whereby the binding of one ligand enhances the affinity or accessibility of binding sites for the other ligand. This cooperative binding could lead to synergistic changes in the protein's structure or microenvironment, resulting in the observed decrease in absorption intensity and red shift in both absorption peaks.

In conjunction with the UV–vis absorption data, circular dichroism (CD) spectroscopy offers valuable insights into the structural alterations induced by CTAB, dicloxacillin, and their combination on fibrinogen. The observed changes in absorption peaks at 214 nm and 280 nm correspond to alterations in protein conformation and the microenvironment surrounding aromatic residues, as evidenced by the CD spectra. The decrease in absorption intensity at 214 nm, indicative of alterations in α-helix structures, correlates with the decrease in α-helix content observed in the CD spectra upon ligand binding. This suggests that the disruption or stabilization of α-helix motifs within fibrinogen, as inferred from the absorbance data, is accompanied by corresponding changes in protein secondary structure, as revealed by CD spectroscopy.

Furthermore, the synergistic effects observed in the CD spectra, characterized by significant alterations in protein secondary structure upon the combined addition of CTAB and dicloxacillin, parallel the synergistic changes observed in the UV–vis absorption data. This suggests that the combined presence of CTAB and dicloxacillin induces cooperative effects on fibrinogen conformation, resulting in more pronounced alterations in protein structure compared to individual ligand treatments. The interaction of the cationic mixture, comprising CTAB and dicloxacillin, with the protein fibrinogen is likely to involve specific binding sites and molecular interactions that influence protein conformation. CTAB, being a cationic surfactant, primarily interacts with fibrinogen through electrostatic interactions due to its positively charged nature. These interactions can occur with negatively charged residues, such as glutamic acid (Glu) and aspartic acid (Asp), which are abundant in protein structures. Furthermore, the hydrophobic alkyl chains of CTAB can associate with non-polar regions of fibrinogen, thereby contributing to the overall stability of the ligand-protein complex. Conversely, dicloxacillin may form noncovalent bonds with specific amino acid residues within fibrinogen, including cysteine (Cys) residues or other nucleophilic residues susceptible to nucleophilic attack. Such interactions may result in localized structural rearrangements within fibrinogen, which could influence its overall conformation. When both CTAB and dicloxacillin are present in the cationic mixture, they may compete for binding sites on the fibrinogen protein, potentially leading to altered ligand-protein interactions compared to

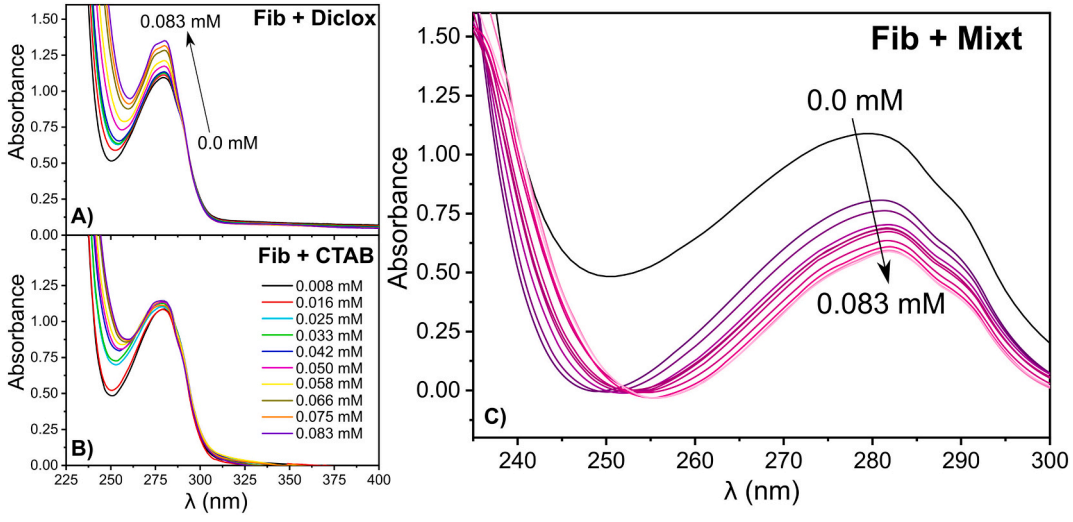

Fig. 4. On the left, a graphical representation of the absorption spectra for the fibrinogen protein showing details on the variation of the absorption peak at 280 nm under the different spectroscopic conditions evaluated with the isolated ligands: A) Fib plus Diclox and B) Fib plus CTAB. Please note that for both spectroscopic conditions mentioned above, increasing concentrations ranging from 0.008 to 0.083 mM were established. Here, the reference control is represented by the absorption spectra labeled in black for the fibrinogen protein (0.07 mM) in the absence of the evaluated ligands (i.e., Diclox or CTAB at a concentration of 0.00 mM) included for comparison purposes. On the right, C) represents the absorption spectra of the fibrinogen plus a mixture of CTAB/Diclox (1:1) (i.e., fib + Mix) with the corresponding reference control represented by the absorption spectra labeled in black for the fibrinogen protein (0.07 mM) in the absence of the evaluated mixture (i.e., mixture CTAB/Diclox at 0.00 mM) included for comparison purposes.

when each ligand is present alone. This competition could result in alterations to the protein's conformational dynamics or stability, which would affect both the absorption peak at 214 nm, which is associated with α-helix structures, and the absorption peak at 280 nm. Furthermore, the cooperative effects observed in the circular dichroism spectra suggest that the binding of one ligand may enhance the affinity or accessibility of binding sites for the other ligand.

The percentage of α-helix can be obtained through the following expression (Eq. (1)) [48]:

$$\propto - helix\ (\%) = \frac{-MRE_{210} - 4000}{33000 - 4000} \times 100 \quad (1)$$

where MRE_{210} represents the observed mean residue ellipticity (MRE) value at 210 nm, with 4000 denoting the MRE of the β-form and random coil conformation cross at 210 nm, and 33,000 indicating the MRE value of the pure α-helix at 210 nm.

While the CD results show a decrease in α-helix content as dicloxacillin concentration increases (Table 1), this does not necessarily contradict the hypothesis that dicloxacillin interacts with fibrinogen in a stabilizing manner at specific structural sites. The observed reduction in α-helix content could indicate that dicloxacillin induces local structural rearrangements that lead to the unfolding or alteration of the fibrinogen secondary structure. This behavior is consistent with the notion that dicloxacillin forms strong non-covalent interactions with certain amino acids, promoting conformational changes that may disrupt the native α-helix configuration. The increase in absorption at 214 nm, while indicating changes in protein structure, reflects a complex interaction that may involve both stabilization of certain motifs and disruption of others, particularly as concentration increases. Thus, the data align with the idea that dicloxacillin induces significant structural modifications, but these modifications may not exclusively restore or stabilize the α-helix structure across all conditions.

To continue the analysis and to further investigate supramolecular protein-ligand interactions, changes in fluorescence spectroscopy were studied. Fluorescence offers a detailed view into the structural changes occurring within proteins upon ligand binding, particularly by monitoring the fluorescence emitted by aromatic amino acid residues like tryptophan (Trp) and tyrosine (Tyr), which in the case of fibrinogen, contribute significantly to its fluorescence spectrum.

Upon examination of the interaction between fibrinogen and CTAB (Fig. 5), it is plausible to suggest that CTAB molecules may interact with charged or polar residues on the protein surface. This interaction may alter the microenvironment surrounding the aromatic residues, leading to changes in fluorescence intensity. When CTAB is introduced to fibrinogen, an increase in fluorescence intensity is observed. This increase can be attributed to several factors, including the unfolding of the protein's tertiary structure induced by weak electrostatic and strong hydrophobic interactions between fibrinogen and CTAB. Fibrinogen possesses a net negative charge due to its composition, containing numerous protonated acidic residues and fewer deprotonated basic residues. Conversely, CTAB is positively charged, facilitating weak electrostatic interactions with the negatively charged residues on the fibrinogen surface. Furthermore, the hydrophobic portions of CTAB may

Table 1
Contents (in %) of the α-helices elements in fibrinogen upon the addition of dicloxacillin and the mixture CTAB/Diclox.

[Ligand] (mM)	α – Helix (%)	
	Diclox	CTAB/Diclox
0	39.98	39.98
0.083	35.86	26.31
0.16	32.70	21.57
0.25	29.58	17.54
0.33	27.66	9.79
0.42	26.24	4.82

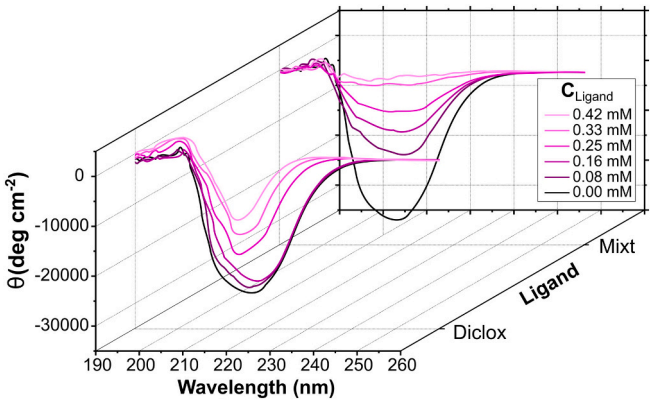

Fig. 5. Graphical representation of the Far-UV CD spectra obtained for the two spectroscopic conditions evaluated: i) Fib plus Diclox (spectra in the foreground as labeled-purple lines) and ii) fibrinogen plus a mixture of CTAB/Diclox (1:1) (spectra in the background as labeled-purple lines). Please note that for both spectroscopic conditions mentioned above, increasing concentrations ranging from 0.08 to 0.42 mM were established. Herein, the reference control is fibrinogen (0.07 mM) in the absence of the evaluated ligands (i.e., Diclox or the mixture CTAB/Diclox both at 0.00 mM) and was included for comparison purposes.

interact with hydrophobic regions within the protein structure, thereby further stabilizing the CTAB-fibrinogen complex. Similarly, dicloxacillin could interact with specific amino acid residues within fibrinogen, potentially through hydrogen bonding or hydrophobic interactions. These interactions could lead to conformational changes in the protein structure, resulting in fluorescence quenching. In this context, the Stern-Volmer approach holds significant importance in studying systems involving proteins and ligands, as this approach allows for the quantification and characterization of the quenching process, which is vital for understanding the interactions between the protein and the ligands at a molecular level.

The Stern-Volmer equation is particularly useful in elucidating the nature of the quenching mechanism. When a ligand is introduced, the Stern-Volmer equation can reveal whether the quenching process follows a dynamic or static mechanism. In the case of dynamic quenching, collisions between the fluorophore (in this instance, fibrinogen) and the quencher (dicloxacillin) result in a decrease in fluorescence intensity. In contrast, static quenching is characterized by the formation of a non-fluorescent complex between the fluorophore and the quencher. Finally, mixed quenching arises from a combination of both collision and complex formation. To elucidate the underlying mechanism, the Stern-Volmer equation is employed [49]:

$$F_0/F = 1 + K_{sv}[Q] = 1 + k_q\tau_0[Q] \quad (2)$$

where F_0 and F represent the fluorescence intensities in the absence and presence of the quencher, respectively. The Stern-Volmer quenching constant (Ksv) is employed to ascertain the quenching mechanism, while the biomolecular quenching constant (kq) quantifies the rate at which the quencher interacts with the fluorophore. An essential parameter for determining quenching efficiency is the excited state lifetime (τ_0) of the biomolecule in the absence of the quencher. Experimentally determined, τ_0 is specific to the fluorophore under study. For fibrinogen, τ_0 was used as 7.208 ns as recently experimentally probed [48].

Furthermore, the addition of a mixture of dicloxacillin and CTAB to the system renders the Stern-Volmer approach even more crucial. The observed deviation from linearity in the Stern-Volmer plot indicates a departure from a simple static or dynamic quenching model. Instead, it suggests the presence of additional, more complex interactions between the fluorophore (fibrinogen) and the quenchers (dicloxacillin and CTAB). These interactions may involve changes in the

microenvironment of the fluorophore, alterations in protein conformation, or the formation of multiple quenching complexes.

Fig. 6E displays a Stern-Volmer plot of F_0/F against [Q]. For either purely dynamic (K = 0) or purely static (k = 0) quenching, the plot manifests linearity, while combined quenching yields an upward curvature. In this scenario, the system between fibrinogen and dicloxacillin is well adjusted to a linear fit ($R^2 = 0.978$), while with the addition of the mixture of ligands, especially at higher concentrations, the plot notably deviates from linearity. This fact signifies a coexistence of interactions between fibrinogen, dicloxacillin and CTAB in both the ground and first excited single states, corresponding to static and dynamic quenching, respectively. Consequently, accounting for the product of static and dynamic quenching, the intensity ratio F_0/F can be more precisely described by the equation:

$$F_0 \big/ F = (1 + K_{SV}[Q])(1 + K_g[Q]) = 1 + (K_{SV} + K_g)[Q] + (K_{SV}K_g)[Q]^2 \quad (3)$$

Here, K_{SV} and K_g are the dynamic quenching constant and ground-state association constant of the complex, respectively. In Fig. 6e at higher quencher concentrations, the Stern-Volmer plot exhibits a continuous ascending curve. A quadratic least square fit proves suitable in this instance, with a correlation constant close to 1 ($R^2 = 0.991$). The obtained K_{SV} from the slope for the system Fib-Diclox at 298 K was (8.87 ± 0.09) × 10^3 L mol^{-1}, corresponding to a quenching constant (k_q) of (1.23 ± 0.03) × 10^{12} M^{-1} s^{-1}. Regarding the mixed ligands, the individual values for K_{SV} and K_g can be obtained from the two solutions of the quadratic (Eq. (3)). In this case, the respective values for the constants were 8.74 ± 0.03 and 2.91 ± 0.01, with the K_g being substantially smaller than the K_{SV}. By analyzing this condition alongside the measured values of kq, it is possible to identify the host-guest interaction mechanism. When the interaction is predominantly diffusion-controlled, the values of kq for dynamic quenching typically fall within the range of 1 × 10^{10} M^{-1} s^{-1}. If the values exceed this limit, it can be inferred that the interaction is static quenching. For both systems, Fib-Diclox and Fib-CTAB/Diclox, the quenching rate constant is significantly greater than the maximum diffusion rate limit. Therefore, it can be concluded that the interaction is a static quenching process resulting from complex formation. Additionally, the Ka value of CTAB/Diclox and fibrinogen mixture decreases as temperature increases, indicating that higher temperatures reduce the stability of these association complexes. This suggests that the binding reactions between the ligands and fibrinogen are exothermic. This conclusion is further supported by the enthalpy change data presented in Table 3.

3.2.2. *Binding parameters*

In the context of static quenching, it is assumed that the protein's binding sites are identical and independent, meaning each site binds the ligand with the same affinity. This binding process can be described by a series of equilibrium steps, where each successive ligand molecule binds to the protein, forming complexes of increasing size (more details can be found in the SI). By analyzing the changes in fluorescence intensity, we can calculate the binding constants (K_A) and determine the number of binding sites (n) on the protein.

The data shows that the fluorescence intensity changes with the

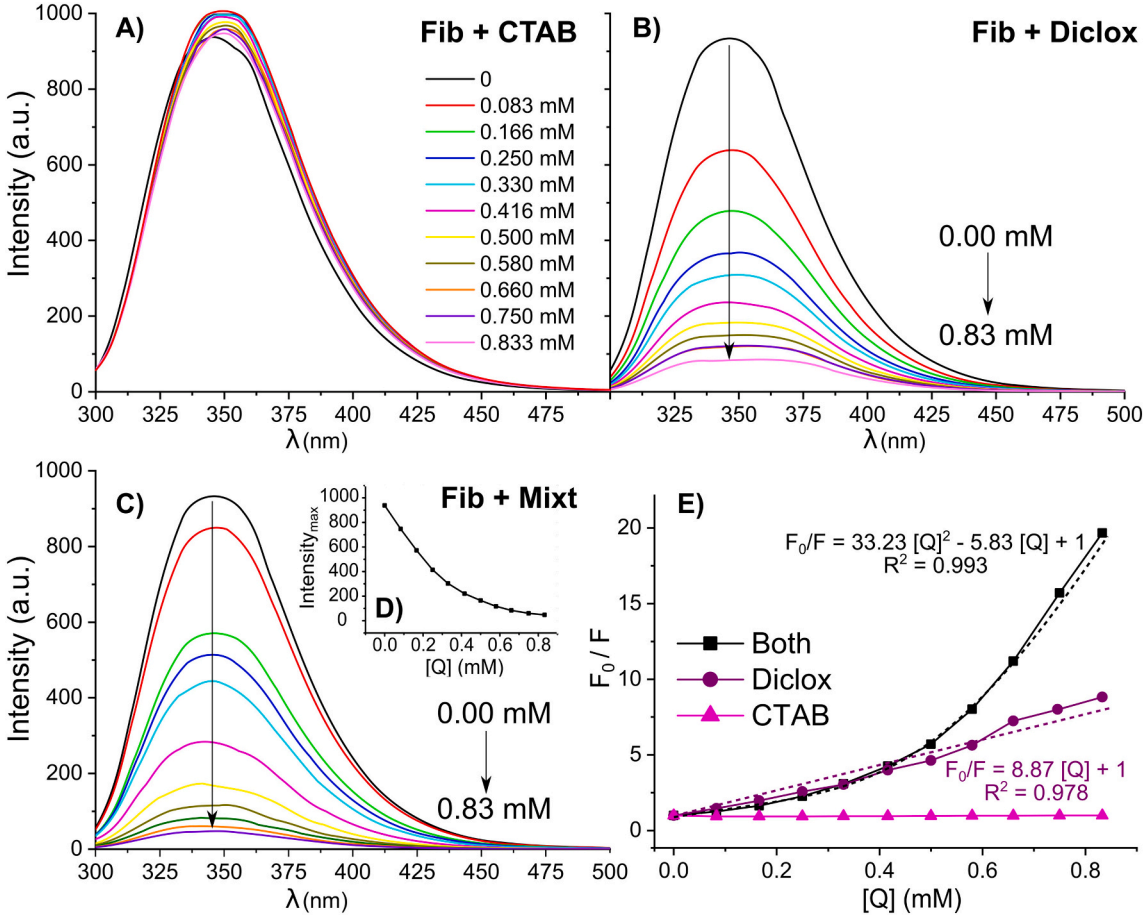

Fig. 6. Emission spectra of fibrinogen (C_{Fib} = 0.07 mM) in the absence and presence of the ligands A) CTAB, B) Diclox and C) Mixture of dicloxacillin and CTAB combined. The black line in the spectra corresponds to the reference control, which consists of fibrinogen (0.07 mM) without Diclox or the CTAB/Diclox mixture (both at 0.00 mM) and is included for comparison. D) Maximum intensity variation as a function of the concentration of the ligand added. E) Stern Volmer plot for the three studied systems. $C_{Diclox} = C_{CTAB}$ = (0.083, 0.166, 0.250, 0.330, 0.416, 0.500, 0.580, 0.660, 0.750, 0.830 mM.

concentration of ligand and protein, and the relationship follows a linear pattern ($R < 0.98$) (Fig. 7b), indicating that the interaction between dicloxacillin and CTAB/Diclox with fibrinogen aligns well with the site-binding model described by Eq. (SI1). This suggests the presence of a single class of binding sites on the fibrinogen molecule for these ligands. Examining the experimental data reveals that the average number of binding sites (n) in both systems is close to 1. Specifically, the complex of fibrinogen with dicloxacillin exhibits a value of 0.72 ± 0.01, while the catanionic complex of fibrinogen with CTAB/Diclox yields a value of 0.84 ± 0.01. This indicates the presence of a predominant binding site for both scenarios. Moreover, the binding affinities are on the order of 10^4 strongly implying that the drug's affinity for the biomacromolecule is moderate.

Computational results of the conformational isobologram (Fig. 2C) have provided a detailed theoretical framework suggesting that the interaction of the mixture may vary depending on specific conformations, with some binding modes showing strong to moderate antagonistic effects, while others show moderate to strong synergistic effects. This variability suggests the complexity of allosteric interactions, where different ligand-binding conformations alter the overall binding mechanisms of fibrinogen. These theoretical predictions can be verified by analyzing the experimental data in Table 2. In this sense, the static quenching dominance indicates the formation of non-fluorescent complexes between fibrinogen and the mixture. This is also in good agreement with the computational prediction of stable docking complexes. The observed static quenching suggests that the conformational changes induced by the mixture are likely to result in binding modes that stabilize the fibrinogen-ligand complex, as evidenced by the higher frequency of binding events in the mixture system in the theoretical docking results. In addition, the Hill coefficient (n) derived from both the computational predictions and the experimental data suggests positive allosteric cooperativity in the binding process. The computational results indicate that conformational changes may lead to positive allosteric effects, especially in the E and D regions, which is supported by the experimental binding parameters. The near-unity binding site numbers and moderate binding affinities suggest that the binding of fibrinogen to CTAB and dicloxacillin involves a single predominant binding site, further supporting the theory that specific conformations of the mixture enhance the overall interaction with fibrinogen. The non-linear behavior observed in the Stern-Volmer plots, especially at higher concentrations, reinforces the idea of conformational diversity in the ligand-protein interaction highlighted in the isobologram analysis. The experimental data showing a combination of static and dynamic quenching probably reflect the dual binding mechanism of the mixture, where different conformations induce either synergistic or antagonistic effects, depending on the concentration and the conformational state of the

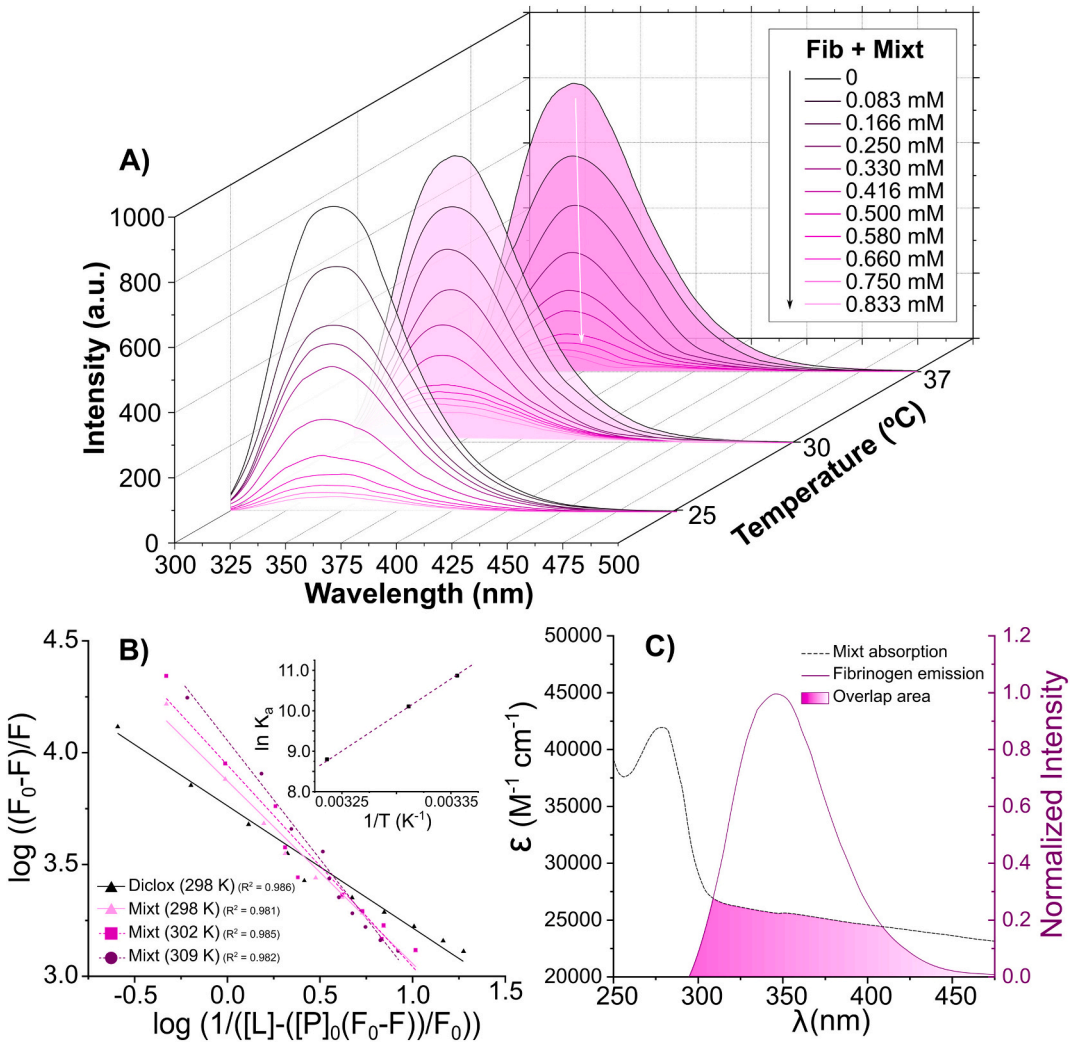

Fig. 7. A) Fluorescence spectra of fibrinogen with increasing concentrations of the mixture of ligands at three different temperatures (298 K, 302 K and 309 K). B) Results of the fittings for the Eq. (12). Inset: Fitting for the obtention of the thermodynamic parameters. C) Overlap of fluorescence emission spectrum (J(λ), pink area) of fibrinogen (purple line) and absorption spectrum of the mixture of CTAB and Diclox (dotted line). $T = 298$ K. $C_{Fib} = 0.07$ mM, $C_{CTAB} = C_{Diclox} = 0.5$ mM.

Table 2
Stern-Volmer quenching constants and binding parameters for the interaction of fibrinogen with dicloxacillin and the mixture CTAB/dicloxacillin at 298 K.

Ligands (temperature)	Stern-Volmer constants				Binding parameters		
	10^{-3} Ksv (mol^{-1})	10^{-3} kg (mol^{-1})	10^{-12} kq (mol^{-1} s^{-1})	R^2	n	10^4 K_A (mol^{-1})	R^2
Diclox (298 K)	8.87 ± 0.09	–	1.23 ± 0.03	0.978	0.78 ± 0.02	8.63 ± 0.03	0.986
Mixt (298 K)	8.74 ± 0.03	2.91 ± 0.01	1.21 ± 0.02	0.993	0.82 ± 0.04	5.24 ± 0.07	0.981
Mixt (302 K)	–	–	–	–	0.90 ± 0.05	2.45 ± 0.03	0.985
Mixt (309 K)	–	–	–	–	1.06 ± 0.07	0.66 ± 0.06	0.982

protein-ligand complex.

Based on the current findings, the role of allosteric interactions and conformational changes in modulating the binding behavior of fibrinogen is closely related to observations in the existing literature. For example, previous studies [50] emphasize that cooperativity in non-covalent interactions, such as hydrogen bonding, enhances molecular stability and significantly influences conformational landscapes. In this study, the observed static quenching dominance and the formation of stable non-fluorescent complexes suggest that the binding of fibrinogen to the mixture, including CTAB and dicloxacillin, is stabilized by these weak but cooperative interactions, leading to conformational changes. These changes are in good agreement with the theoretical prediction of positive allosteric cooperativity. Another interesting study [51] showed that allosteric regulation, through subtle but crucial conformational shifts, can either enhance or inhibit enzymatic activity. In the context of the fibrinogen-ligand interaction, the different computationally predicted binding modes, ranging from antagonistic to synergistic effects, reflect this complexity of allosteric modulation. The non-linear behavior in the Stern-Volmer plots supports the hypothesis that the mixture induces distinct conformational states that either facilitate or inhibit binding, depending on the concentration and protein-ligand conformational alignment. This non-linear binding behavior may reflect a mechanism similar to uncompetitive inhibition, where certain conformations selectively promote synergistic binding. The dynamic nature of these interactions is further emphasized by the findings of how conformational flexibility in malaria vaccine antigenic proteins affects their immunogenicity [52]. The dual binding mechanism observed in the current system, where both static and dynamic quenching occur, suggests that fibrinogen undergoes a similar conformational flexibility. This flexibility may allow the protein to adopt multiple binding conformations, which in turn may influence the observed synergistic or antagonistic effects observed. The predicted positive allosteric cooperativity in the E and D regions of fibrinogen likely arises from this conformational plasticity, mirroring the antigen-protein interactions described by Ragotte et al. [52]. In addition, the findings from Minnelli et al. [53] highlight how membrane components undergo allosteric changes due to amphiphilic molecules, leading to increased permeability and destabilization. Although the current system involves fibrinogen, the mechanism of action may be analogous, with the amphiphilic nature of CTAB inducing conformational changes that stabilize the fibrinogen-ligand complex. This is supported by the experimental binding affinities and Hill coefficients suggesting that specific conformations enhance the interaction.

3.2.3. Thermodynamic parameters and binding forces

Thermodynamic parameters such as enthalpy change (ΔH), entropy change (ΔS), and free energy change (ΔG) play a crucial role in elucidating the interaction mechanism. If ΔH remains relatively constant over the temperature range being studied, it can be considered as a constant. The Van't Hoff equation (Eq. (4)) allows the evaluation of ΔH and ΔS using the binding constant (K_A) at different temperatures, where R represents the gas constant:

$$lnK_A = -\frac{\Delta H}{RT} + \frac{\Delta S}{R} \quad (4)$$

By examining the linear relationship between ln Ka and 1/T, the slope yields ΔH, and the intercept provides ΔS (Fig. 7b). The values of ΔG can be obtained then using the thermodynamic expression:

$$\Delta G = \Delta H - T\Delta S \quad (5)$$

Negative ΔG and ΔH values indicate that the binding process of ligands to fibrinogen is a spontaneous exothermal reaction. ΔG reflects the combined effects of ΔH and ΔS. Negative ΔH and ΔS values suggest that the interaction between fibrinogen and the mixture of CTAB and dicloxacillin is primarily enthalpy-driven, with entropy contributing unfavourably to the spontaneity of the reaction. The negative ΔS value may reflect a reduction in configurational freedom within the system, potentially due to structural reorganization in the fibrinogen molecule or the formation of highly ordered molecular complexes. Noncovalent interaction forces such as van der Waals forces, hydrophobic interactions, electrostatic interactions, and hydrogen bonds are known to mediate the interaction between small molecules and biomacromolecules. In this context, the observed decrease in entropy could result from specific interactions, such as hydrogen bonding or electrostatic interactions, which impose a more constrained configuration on the system.

The formation of a hydrophobic cavity within the fibrinogen molecule facilitates the interaction with drug molecules, inducing an exothermic process. In addition, electrostatic forces between CTAB/Diclox and fibrinogen may also contribute to the exothermic effects. The negative ΔH value suggests the involvement of hydrophobic interactions and electrostatic forces, with the possible formation of intermolecular hydrogen bonds facilitated by hydroxyl groups on the backbone of the ligand mixture.

Table 3
The thermodynamic parameters of the interaction between fibrinogen and the catanionic mixture at different temperatures.

	Thermodynamic parameters			
	T (K)	ΔG (kJ mol^{-1} K^{-1})	ΔH (kJ mol^{-1})	ΔS (J mol^{-1} K^{-1})
Mixt	298	−26.942	−144.131	
	302	−25.369		−393.252
	309	−22.616		

Table 4
Fluorescence resonance energy transfer (FRET) results of fibrinogen with the mixture CTAB/~~d~~ Diclox.

	FRET parameters		
	J (M^{-1} cm^{-1} nm^4)	R_0 (Å)	r (nm)
CTAB/Diclox	4.036×10^{14}	36.29	5.17

3.2.4. FRET

The study of energy transfer provides valuable insights into the interactions between fibrinogen and catanionic ligands. Fluorescence resonance energy transfer (FRET) has become a widely used tool for investigating protein-ligand interactions and changes in protein structure upon ligand binding [54]. This non-invasive technique allows the observation of energy transfer from an excited donor molecule (fibrinogen) to an acceptor molecule (catanionic ligands), without the

emission of radiation. In FRET, the donor typically emits at shorter wavelengths that overlap with the acceptor's absorption spectrum. For effective energy transfer to occur, certain conditions must be met: (i) the donor must be fluorescent, (ii) the spectral overlap between the donor's emission and the acceptor's absorption should be significant (Fig. 7C), and (iii) the distance between the donor and acceptor must be sufficiently small, generally <7 nm. These criteria ensure the likelihood of energy transfer and make it possible to estimate the proximity between fibrinogen's key residues and the interacting ligands [55]. (For a more detailed explanation of the theoretical aspects of the FRET analysis, please refer to the SI). In the present case, FRET analysis helps to assess the spatial arrangement and binding dynamics. The efficiency of energy transfer can be used to deduce the conformational changes occurring in the protein upon binding. Since the interaction between fibrinogen and ligands is characterized by the formation of a non-fluorescent complex, the observed energy transfer strongly suggests that a static quenching mechanism dominates the interaction. This is in line with the idea that fibrinogen undergoes structural rearrangements upon binding, leading to a reduction in fluorescence intensity.

Furthermore, the calculated transfer distances (Table 4) indicate that the binding sites of catanionic ligands are in close proximity to the protein's fluorescent residues, making energy transfer highly probable. The observed energy transfer efficiency highlights the non-radiative nature of the process, where excitation energy is effectively transferred from the donor to the acceptor molecules. These results support the hypothesis that the binding between fibrinogen and catanionic ligands is characterized by strong, specific interactions that likely induce changes in the protein's conformation.

4. Conclusions

This study combines theoretical docking and experimental approaches to elucidate the interactions between fibrinogen and the CTAB-dicloxacillin mixture, revealing both synergistic and antagonistic effects across specific binding regions. Theoretical predictions identified the D-regions as sites of synergistic interactions and the E-region as a site of antagonistic effects, aligning with experimental data from UV–vis and fluorescence spectroscopy that indicated distinct binding mechanisms. Notably, CTAB disrupted the α-helix structure of fibrinogen, while dicloxacillin stabilized it, reflecting the region-specific effects predicted by docking studies. Additionally, both experimental and theoretical results suggest that the ligand mixture forms more stable complexes than the individual ligands. FRET analysis confirmed the close proximity of ligands to fibrinogen's fluorescent residues, supporting specific binding interactions, while thermodynamic analysis revealed spontaneous, exothermic binding driven by hydrophobic and electrostatic forces. The non-linear behavior observed in Stern-Volmer plots and isobologram models emphasizes the complex, cooperative interactions within this ligand system, providing a detailed understanding of how mixed ligand systems like CTAB and dicloxacillin modulate fibrinogen structure through synergistic and antagonistic effects, which offers a valuable framework for future studies on protein-ligand interactions and modulation.

While these findings offer valuable insights, the study is limited by the fact that the in vitro conditions may not fully replicate the complexities of physiological environments. Further studies are necessary to investigate the impact of these interactions on clot formation, drug bioavailability, and toxicity in real biological systems. Nonetheless, the strength of this study lies in the comprehensive approach combining molecular docking and various spectroscopic techniques, providing a thorough understanding of the binding mechanisms and structural alterations induced by the ligand mixture. These results contribute to the growing knowledge on protein-ligand interactions, offering a valuable framework for the future design of drug delivery systems and exploring new therapeutic strategies.

Declaration of Generative AI and AI-assisted technologies

During the preparation of this work the author(s) used ChatGPT by OpenAI in order to improve language and readability. After using this tool/service, the author(s) reviewed and edited the content as needed and take(s) full responsibility for the content of the publication.

CRediT authorship contribution statement

Ramón Rial: Writing – review & editing, Writing – original draft, Methodology, Formal analysis, Data curation, Conceptualization. **Michael González-Durruthy:** Writing – review & editing, Writing – original draft, Software, Methodology, Conceptualization. **Juan M. Ruso:** Writing – review & editing, Supervision, Conceptualization.

Declaration of competing interest

The authors declare the following financial interests/personal relationships which may be considered as potential competing interests: Juan M. Ruso reports financial support was provided by the Government of Galicia. Ramon Rial reports a relationship with Government of Spain Ministry of Universities that includes: funding grants. If there are other authors, they declare that they have no known competing financial interests or personal relationships that could have appeared to influence the work reported in this paper.

Acknowledgements

R.R., M.G.D, and J.M.R. thank Xunta de Galicia for support (ED431B 2022/36). R.R. is granted by the Program for the requalification, international mobility, and attraction of talent in the Spanish University System, modality Margarita Salas (grant UP2021-042).

Appendix A. Supplementary data

Supplementary data to this article can be found online at https://doi.org/10.1016/j.ijbiomac.2025.140265.

Data availability

Data will be made available on request.

References

[1] O.M. Salo-Ahen, I. Alanko, R. Bhadane, A.M. Bonvin, R.V. Honorato, S. Hossain, A. H. Juffer, A. Kabedev, M. Lahtela-Kakkonen, A.S. Larsen, Molecular dynamics simulations in drug discovery and pharmaceutical development, Processes 9 (1) (2020) 71.
[2] S. Waheed, Z. Li, F. Zhang, A. Chiarini, U. Armato, J. Wu, Engineering nano-drug biointerface to overcome biological barriers toward precision drug delivery, J. Nanobiotechnol. 20 (1) (2022) 395.
[3] R. Rial, M. González-Durruthy, Z. Liu, R.L. Reis, J.M. Ruso, Revealing the binding dynamics between catanionic surfactants and lysozyme: a synergistic computational approach coupled with experimental validation, J. Mol. Liq. 390 (2023) 123121.
[4] M. González-Durruthy, R. Rial, Z. Liu, J.M. Ruso, Lysozyme allosteric interactions with β-blocker drugs, J. Mol. Liq. 366 (2022) 120370.
[5] D. Otzen, Protein–surfactant interactions: a tale of many states, Biochimica et Biophysica Acta (BBA)-Proteins and Proteomics 1814 (5) (2011) 562–591.
[6] M. Aguirre-Ramírez, H. Silva-Jiménez, I.M. Banat, M. Díaz De Rienzo, Surfactants: physicochemical interactions with biological macromolecules, Biotechnol. Lett. 43 (3) (2021) 523–535.
[7] R. Rial, M. González-Durruthy, M. Somoza, Z. Liu, J.M. Ruso, Unraveling the compositional and molecular features involved in lysozyme-benzothiazole derivative interactions, Molecules 26 (19) (2021) 5855.
[8] M. González-Durruthy, R. Rial, M.N.D.S. Cordeiro, Z. Liu, J.M. Ruso, Exploring the conformational binding mechanism of fibrinogen induced by interactions with penicillin β-lactam antibiotic drugs, J. Mol. Liq. 324 (2021) 114667.
[9] J. Maldonado-Valderrama, A. Martín-Molina, A. Martín-Rodriguez, M. A. Cabrerizo-Vílchez, M.J. Gálvez-Ruiz, D. Langevin, Surface properties and foam stability of protein/surfactant mixtures: theory and experiment, J. Phys. Chem. C 111 (6) (2007) 2715–2723.

[10] J. Maldonado-Valderrama, J.M.R. Patino, Interfacial rheology of protein–surfactant mixtures, Curr. Opin. Colloid Interface Sci. 15 (4) (2010) 271–282.
[11] R. Miller, V.B. Fainerman, M.E. Leser, M. Michel, Surface tension of mixed non-ionic surfactant/protein solutions: comparison of a simple theoretical model with experiments, Colloids Surf. A Physicochem. Eng. Asp. 233 (1) (2004) 39–42.
[12] C. Kotsmar, V. Pradines, V.S. Alahverdjieva, E.V. Aksenenko, V.B. Fainerman, V. I. Kovalchuk, J. Krägel, M.E. Leser, B.A. Noskov, R. Miller, Thermodynamics, adsorption kinetics and rheology of mixed protein–surfactant interfacial layers, Adv. Colloid Interface Sci. 150 (1) (2009) 41–54.
[13] A. Stenstam, A. Khan, H. Wennerström, Lysozyme in catanionic surfactant mixtures, Langmuir 20 (18) (2004) 7760–7765.
[14] J.X. Xiao, U. Sivars, F. Tjerneld, Phase behavior and protein partitioning in aqueous two-phase systems of cationic–anionic surfactant mixtures, Journal of Chromatography. B, Biomedical Sciences and Applications 743 (1–2) (2000) 327–338.
[15] E. Blanco, P. Messina, J.M. Ruso, G. Prieto, F. Sarmiento, Regarding the effect that different hydrocarbon/fluorocarbon surfactant mixtures have on their complexation with HSA, J. Phys. Chem. B 110 (23) (2006) 11369–11376.
[16] S. Shahraki, H.S. Delarami, Z. Razmara, A. Heidari, Tracking the binding site of anticancer drug fluxoridin with Fe-related proteins to achieve intelligent drug delivery, Spectrochim. Acta A Mol. Biomol. Spectrosc. 306 (2024) 123569.
[17] O. Barani, S. Shahraki, Z. Sori Nezami, H. Samareh Delarami, E. Sanchooli, Unveiling the molecular association of novel benzohydrazide-substituted Schiff base complexes with human serum albumin, Inorg. Chem. Commun. 162 (2024) 112200.
[18] A. Oveisi Keikha, S. Shahraki, E. Dehghanian, H. Mansouri-Torshizi, Effect of central metal ion on some pharmacological properties of new Schiff base complexes. Anticancer, antioxidant, kinetic/thermodynamic and computational studies, Spectrochim. Acta A Mol. Biomol. Spectrosc. 325 (2025) 125034.
[19] F. Shahriari, S. Shahraki, E. Dehghanian, Diacetyl monoxime-based N∩N donor Schiff base and its Zn(II) complexes. In vitro and in silico analysis, Applied Organometallic Chemistry 39 (1) (2025) e7763.
[20] L. Xu, L. Feng, S. Dong, J. Hao, Q. Yu, Carbon nanotubes modified by a paramagnetic cationic surfactant for migration of DNA and proteins, Colloids Surf. A Physicochem. Eng. Asp. 559 (2018) 201–208.
[21] J.W. Weisel, R.I. Litvinov, Fibrin formation, structure and properties, in: D.A. D. Parry, J.M. Squire (Eds.), Fibrous Proteins: Structures and Mechanisms, Springer International Publishing, Cham, 2017, pp. 405–456.
[22] C. Chen, S. Zhang, X. Cheng, Y. Ren, Y. Qian, C. Zhang, M. Chen, N. Sun, H. Liu, Reducing cherry rain-cracking: enhanced wetting and barrier properties of chitosan hydrochloride-based coating with dual nanoparticles, Int. J. Biol. Macromol. 268 (2024) 131660.
[23] N. Hassan, L.R. Barbosa, R. Itri, J.M. Ruso, Fibrinogen stability under surfactant interaction, J. Colloid Interface Sci. 362 (1) (2011) 118–126.
[24] T.B. Stage, M. Graff, S. Wong, L.L. Rasmussen, F. Nielsen, A. Pottegård, K. Brøsen, D.L. Kroetz, S.C. Khojasteh, P. Damkier, Dicloxacillin induces CYP2C19, CYP2C9 and CYP3A4 in vivo and in vitro, Br. J. Clin. Pharmacol. 84 (3) (2018) 510–519.
[25] P.L. Mar, R. Gopinathannair, B.E. Gengler, M.K. Chung, A. Perez, J. Dukes, M. D. Ezekowitz, D. Lakkireddy, G.Y.H. Lip, M. Miletello, P.A. Noseworthy, J. Reiffel, J.E. Tisdale, B. Olshansky, Drug interactions affecting oral anticoagulant use, Circ. Arrhythm. Electrophysiol. 15 (6) (2022) e007956.
[26] A. Sangeetha, L. Samyuktha, K. Atya, H. Neha, K.S. Rakesh, G.U. Shantveer, J. Kaiser, Evaluation of biological effects and toxicity of cetyltrimethylammonium bromide stabilized silver nanoparticles and cetyltrimethylammonium bromide alone following intravenous injection in mice, Current Nanomedicine 11 (1) (2021) 70–80.
[27] X. Geng, Y. Wei, Y. Li, S. Zhao, Z. Li, H. Li, C. Li, Antimicrobial activity of nano-GeO2/CTAB complex against fungi and bacteria isolated from paper, Int. J. Mol. Sci. 25 (24) (2024) 13541.
[28] M. Kalbáčová, M. Verdánová, F. Mravec, T. Halasová, M. Pekař, Effect of CTAB and CTAB in the presence of hyaluronan on selected human cell types, Colloids Surf. A Physicochem. Eng. Asp. 460 (2014) 204–208.
[29] A.M. Silva, C. Martins-Gomes, T.E. Coutinho, J.F. Fangueiro, E. Sanchez-Lopez, T. N. Pashirova, T. Andreani, E.B. Souto, Soft cationic nanoparticles for drug delivery: production and cytotoxicity of solid lipid nanoparticles (SLNs), Appl. Sci. 9 (20) (2019) 4438.
[30] M.S. Valdés-Tresanco, M.E. Valdés-Tresanco, P.A. Valiente, E. Moreno, AMDock: a versatile graphical tool for assisting molecular docking with Autodock Vina and Autodock4, Biol. Direct 15 (1) (2020) 12.
[31] S. Kim, J. Chen, T. Cheng, A. Gindulyte, J. He, S. He, Q. Li, B.A. Shoemaker, P. A. Thiessen, B. Yu, L. Zaslavsky, J. Zhang, E.E. Bolton, PubChem 2023 update, Nucleic Acids Res. 51 (D1) (2022) D1373–D1380.
[32] H.M. Berman, J. Westbrook, Z. Feng, G. Gilliland, T.N. Bhat, H. Weissig, I. N. Shindyalov, P.E. Bourne, The protein data bank, Nucleic Acids Res. 28 (1) (2000) 235–242.
[33] J.M. Kollman, L. Pandi, M.R. Sawaya, M. Riley, R.F. Doolittle, Crystal structure of human fibrinogen, Biochemistry 48 (18) (2009) 3877–3886.
[34] S. Preus, DecayFit—Fluorescence Decay Analysis Software 1.3, FluorTools. http://www.fluortools.com, 2014.
[35] A. Micsonai, É. Moussong, F. Wien, E. Boros, H. Vadászi, N. Murvai, Y.-H. Lee, T. Molnár, M. Réfrégiers, Y. Goto, Á. Tantos, J. Kardos, BeStSel: webserver for secondary structure and fold prediction for protein CD spectroscopy, Nucleic Acids Res. 50 (W1) (2022) W90–W98.
[36] R. Roy, P.V. Murphy, H.-J. Gabius, Multivalent carbohydrate-lectin interactions: how synthetic chemistry enables insights into nanometric recognition, Molecules 21 (5) (2016) 629.
[37] N. Kaviyarasi, Structure, Biosynthesis, and Biological Properties of Lectins, Lectins: Innate Immune Defense and Therapeutics, Springer, 2022, pp. 27–50.
[38] P. Singh, A. Roche, C.F. van der Walle, S. Uddin, J. Du, J. Warwicker, A. Pluen, R. Curtis, Determination of protein–protein interactions in a mixture of two monoclonal antibodies, Mol. Pharm. 16 (12) (2019) 4775–4786.
[39] D.J. Spurgeon, O.A.H. Jones, J.-L.C.M. Dorne, C. Svendsen, S. Swain, S. R. Stürzenbaum, Systems toxicology approaches for understanding the joint effects of environmental chemical mixtures, Sci. Total Environ. 408 (18) (2010) 3725–3734.
[40] J.P. Groten, Mixtures and interactions, Food Chem. Toxicol. 38 (2000) S65–S71.
[41] D.O. Carpenter, K. Arcaro, D.C. Spink, Understanding the human health effects of chemical mixtures, Environ. Health Perspect. 110 (Suppl. 1) (2002) 25–42.
[42] S. Köhler, F. Schmid, G. Settanni, The internal dynamics of fibrinogen and its implications for coagulation and adsorption, PLoS Comput. Biol. 11 (9) (2015) e1004346.
[43] T.-C. Chou, Drug combination studies and their synergy quantification using the Chou-Talalay method, Cancer Res. 70 (2) (2010) 440–446.
[44] S. Zheng, W. Wang, J. Aldahdooh, A. Malyutina, T. Shadbahr, Z. Tanoli, A. Pessia, J. Tang, SynergyFinder plus: toward better interpretation and annotation of drug combination screening datasets, Genomics Proteomics Bioinformatics 20 (3) (2022) 587–596.
[45] A. Ianevski, A.K. Giri, T. Aittokallio, SynergyFinder 2.0: visual analytics of multi-drug combination synergies, Nucleic Acids Res. 48 (W1) (2020) W488–W493.
[46] D.J. Wooten, R. Albert, Synergy: a Python library for calculating, analyzing and visualizing drug combination synergy, Bioinformatics 37 (10) (2020) 1473–1474.
[47] D.J. Wooten, C.T. Meyer, A.L.R. Lubbock, V. Quaranta, C.F. Lopez, MuSyC is a consensus framework that unifies multi-drug synergy metrics for combinatorial drug discovery, Nat. Commun. 12 (1) (2021) 4607.
[48] X. Li, H. Duan, Z. Song, R. Xu, Comparative study on the interaction between fibrinogen and flavonoids, J. Mol. Struct. 1262 (2022) 132963.
[49] J.R. Lakowicz, Principles of Fluorescence Spectroscopy, Springer, 2006.
[50] A.S. Mahadevi, G.N. Sastry, Cooperativity in noncovalent interactions, Chem. Rev. 116 (5) (2016) 2775–2825.
[51] S. Boulton, R. Selvaratnam, J.-P. Blondeau, F. Lezoualc'h, G. Melacini, Mechanism of selective enzyme inhibition through uncompetitive regulation of an allosteric agonist, J. Am. Chem. Soc. 140 (30) (2018) 9624–9637.
[52] R.J. Ragotte, D. Pulido, A.M. Lias, D. Quinkert, D.G. Alanine, A. Jamwal, H. Davies, A. Nacer, E.D. Lowe, G.W. Grime, Heterotypic interactions drive antibody synergy against a malaria vaccine candidate, Nat. Commun. 13 (1) (2022) 933.
[53] C. Minnelli, G. Mangiaterra, E. Laudadio, B. Citterio, S. Rinaldi, Investigation on the synergy between membrane permeabilizing amphiphilic α-hydrazido acids and commonly used antibiotics against drug-resistant bacteria, Molecules 29 (17) (2024) 4078.
[54] A. Kaur, P. Kaur, S. Ahuja, Förster resonance energy transfer (FRET) and applications thereof, Anal. Methods 12 (46) (2020) 5532–5550.
[55] H. Sahoo, Förster resonance energy transfer – a spectroscopic nanoruler: principle and applications, J. Photochem. Photobiol. C Photchem. Rev. 12 (1) (2011) 20–30.